



the society for solid-state
and electrochemical
science and technology

Journal of The Electrochemical Society

Imaging of Defects Contained within n -Alkylthiol Monolayers by Combination of Underpotential Deposition and Scanning Tunneling Microscopy: Kinetics of Self –Assembly

Li Sun and Richard M. Crooks

J. Electrochem. Soc. 1991, Volume 138, Issue 8, Pages L23-L25.
doi: 10.1149/1.2086000

**Email alerting
service**

Receive free email alerts when new articles cite this article - sign up in the box at the top right corner of the article or [click here](#)

To subscribe to *Journal of The Electrochemical Society* go to:
<http://jes.ecsdl.org/subscriptions>

23, 4701 (1984).

9. R. J. Mortimer and D. R. Rosseinsky, *J. Electroanal. Chem.*, **151**, 133 (1983).10. K. P. Rajan and V. D. Neff, *J. Phys. Chem.*, **86**, 4361 (1982).11. S. Sinha, B. D. Humphrey, and A. B. Bocarsly, *Inorg. Chem.*, **23**, 203 (1984).

Imaging of Defects Contained within *n*-Alkylthiol Monolayers by Combination of Underpotential Deposition and Scanning Tunneling Microscopy: Kinetics of Self-Assembly

Li Sun and Richard M. Crooks*

Department of Chemistry and the Center for High Technology Materials, University of New Mexico, Albuquerque, New Mexico 87131

ABSTRACT

A novel method for imaging individual defect structures contained within thin, insulating layers that cover atomically smooth conducting substrates is described. The technique relies upon imaging metal islands electrochemically deposited within defects that penetrate the insulating layer by scanning tunneling microscopy. The method is illustrated by measuring the rate of self-assembly of a monolayer of $\text{CH}_3(\text{CH}_2)_{17}\text{SH}$ on a Au (111) substrate. The results are found to be in accord with those obtained by spectroscopic and contact angle measurements.

Self-organizing chemical systems represent a versatile approach for the rational modification of surfaces (1), and during the past several years considerable effort has been directed towards the synthesis and characterization of ideal, defect-free mono- and multilayers (2-7). However, little emphasis has been placed on the characterization of adventitious defect structures, or on the synthesis of intentionally formed defect structures, because the techniques that are presently used for studying self-assembled organic surfaces generally rely upon the measurement of average properties of an ensemble of molecules or other features attached to surfaces and are therefore not sensitive to individual, submicron features (4, 8-14).

Here, we describe a strategy for examining the structure and geometrical distribution of individual defect sites contained within an organic framework confined to a Au surface. Our approach to this problem is illustrated in Scheme I. First, the Au surface is imaged to insure that it is smooth and free of most defects. Second, a monolayer of *n*-octadecylthiol, $\text{CH}_3(\text{CH}_2)_{17}\text{SH}$, is adsorbed onto the Au surface. Third, Cu metal is underpotentially deposited within defect sites. Fourth, the resulting island structures contained within the organic adlayer are imaged by scanning tunneling microscopy (STM).

We wish to emphasize and clarify two potentially misleading points about Scheme I. First, we do not know if the tip is above or within the organic monolayer during imaging; however, our data are consistent with the notion that the tip penetrates the *n*-alkylthiol framework as shown in Scheme I. Second, we do not fully understand the exact chemical and morphological characteristics of the island structures (see below).

Two important findings result from the work presented here. First, nanometer-scale defects within the organic monolayer can be imaged by electrochemically converting "negative" defect images into "positive" replicas. Second, it is possible to measure the rate of monolayer formation, or more precisely the rate of defect disappearance, by measuring the number of islands as a function of the time allotted for monolayer deposition.

Experimental

Single crystal Au (111) surfaces were prepared by a method similar to that described by Hsu (15). A 0.008 in. Au wire (99.99%, Ted Pella, Incorporated) was heated in a H_2/O_2 flame surrounded by an inert atmosphere until a molten sphere formed at the end of the wire. After solidification, millimeter-scale Au (111) facets formed on the surface; however, surfaces prepared in this way were frequently found to contain defects

consisting of one or two monolayer-deep pits. Chidsey *et al.* demonstrated that electrochemical methods can be used to remove such defects by electrochemically oxidizing Au in the presence of Cl^- (16). We have followed this procedure and STM images obtained prior to adsorption of $\text{CH}_3(\text{CH}_2)_{17}\text{SH}$ indicate that it results in the removal of most surface defects.

Just prior to UPD of Cu, exposed Au on the $\text{CH}_3(\text{CH}_2)_{17}\text{SH}$ -modified surface was cleaned electrochemically by cycling the electrode potential four times between 0.6 and 1.5 V in a solution containing 0.1M HClO_4 and 1 mM $\text{Cu}(\text{ClO}_4)_2$. One final scan from 0.6 to 0 V resulted in UPD of Cu onto the Au surface. The Au electrode was removed from solution at 0 V and rinsed with water prior to STM imaging.

Electrochemical data were obtained using a conventional cell and a Princeton Applied Research Model 173 potentiostat and Model 175 Universal Programmer. Potentials are reported vs. a Ag/AgCl , NaCl (3M) reference electrode. All chemicals were reagent grade and used as received. Water was purified



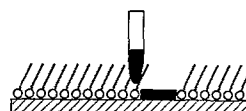
1. The Au (111) facet is imaged by STM to insure that it is flat and defect-free.



2. A single monolayer of an *n*-alkylthiol is adsorbed onto the Au surface from solution. Adventitious defects form in the organic monolayer.



3. Cu metal is underpotentially deposited into the defect sites.



4. The STM is used to image the Cu replicas of the original defect.

Scheme I. Schematic representation of a technique for imaging defect structures contained within an organic monolayer.

* Electrochemical Society Active Member.

by a Milli-Q filtering system (Millipore) and all solutions were degassed with N_2 prior to use. Although STM imaging was performed on Au (111) facets, electrochemical data were necessarily obtained from the primarily polycrystalline surface of the Au balls.

STM images were obtained in air using a NanoScope II STM (17). The following acquisition parameters were generally used: tunneling current, 0.1 nA; bias voltage, 300 mV; scan rate, 1.34 Hz/line; integral gain, 5; proportional gain, 2; feedback mode, constant current; tip material, 80% Pt/20% Ir.

Results and Discussion

We have studied the kinetics of *n*-alkylthiol self-assembly on Au as a proof-of-concept demonstration of the UPD/STM technique. The object of this study is to determine the number density of island structures contained within the organic monolayer, which we correlate with the number of defects originally present, as a function of the time the Au surface is immersed in the $CH_3(CH_2)_{17}SH$ -containing deposition solution.

Self-assembled films of *n*-alkylthiols form highly crystalline $\sqrt{3} \times \sqrt{3}$ ($R30^\circ$) monolayers on Au (111) substrates (14, 18). For this study, monolayers are formed by soaking the Au (111) substrate in an ethanol solution containing 0.5 mM $CH_3(CH_2)_{17}SH$ for times ranging from 10^{-1} to 10^6 min. At the end of the adsorption period, UPD Cu is electrochemically deposited onto accessible regions of the surface following a surface cleaning procedure discussed in the previous section.

The Cu UPD voltammetry (19) for a naked Au substrate and a substrate that was soaked for 6 s in a $CH_3(CH_2)_{17}SH$ -containing ethanol solution is shown in Fig. 1. The integrated cathodic current in Fig. 1b, $50 \mu C/cm^2$, is approximately the same as the integrated anodic stripping current measured after STM imaging, $40 \mu C/cm^2$, indicating that Cu deposited on the surface remains there throughout the imaging process. Figure 1 also shows that the characteristic UPD voltammetry obtained at an *n*-alkylthiol-modified Au substrate is markedly different from that obtained at a naked Au surface. However, theoretical studies have shown that the structure and nature of solvents in very small pores is different than that found in bulk solvents (20), and therefore it is not surprising that some changes are present in the cyclic voltammetry.

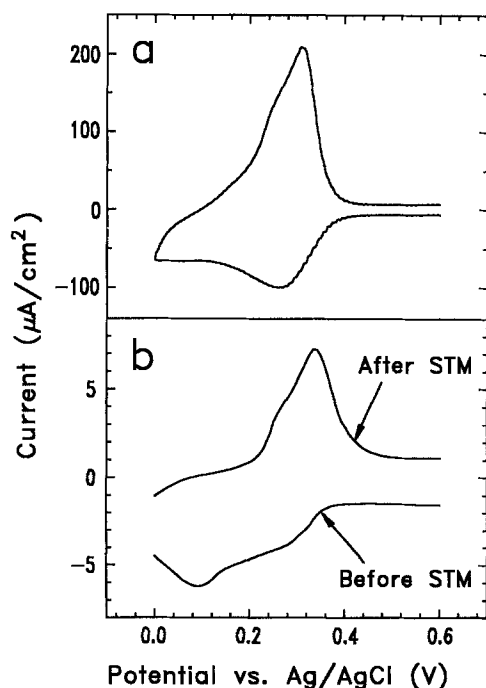


Fig. 1. Voltammetry obtained for the UPD of Cu onto (a) a naked Au substrate; (b) a Au substrate previously soaked for 6 s in an ethanol solution containing 0.5 mM $CH_3(CH_2)_{17}SH$. The cathodic scan in (b) was obtained just prior to STM imaging and the anodic scan was obtained after imaging. The aqueous electrolyte solution contained 0.1M $HClO_4$ and 1 mM $Cu(ClO_4)_2$ and the scan rate was 20 mV/s. All electrochemical experiments were performed on Au balls made according to the procedure described in the text.

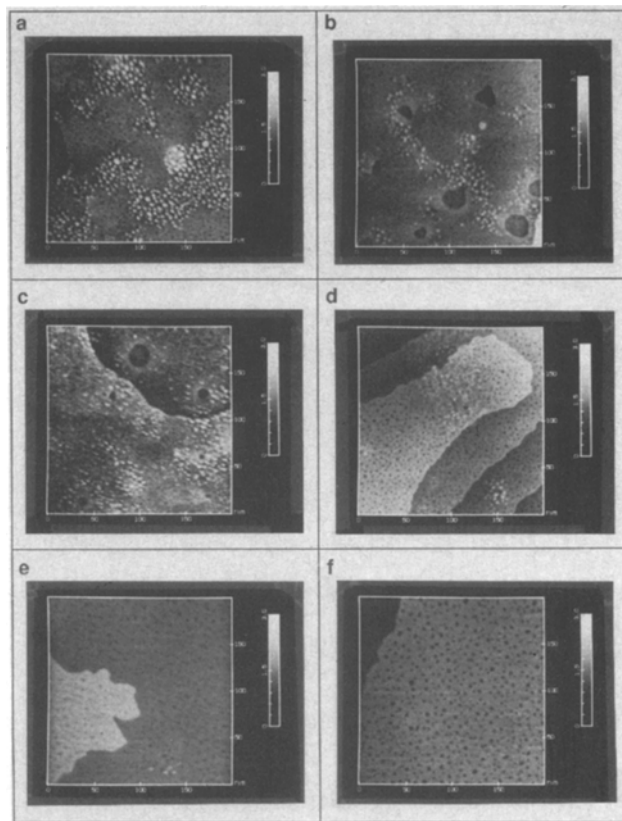


Fig. 2. STM images of Cu UPD islands formed after soaking the Au substrate in an ethanol solution containing 0.5 mM $CH_3(CH_2)_{17}SH$ for (a) 10^{-1} min, (b) 10^0 min, (c) 10^1 min, (d) 10^2 min, (e) 10^3 min, (f) 10^4 min. All images are $200 \text{ nm} \times 200 \text{ nm}$ scans and the z-axis is 3 nm full-scale.

STM images of UPD Cu defect replicas contained within the organic monolayer are shown in Fig. 2. Each frame corresponds to different immersion times ranging from 6 s to about 6 days. Since the Cu islands are formed at potentials positive of that required for bulk Cu deposition, the replicas should be confined to the Au surface and exactly one Cu monolayer thick, about 0.2-0.3 nm. However, STM profile images indicate the islands are typically about 0.6 nm in height. We believe this discrepancy results from changes in the Au surface induced by the electrochemical cleaning step that precedes Cu UPD.

The electrochemical cleaning procedure is necessary to insure that all exposed regions of the Au surface are clean enough to be receptive to Cu UPD. However, electrochemical cleaning has two important effects on the substrate morphology. First, it enlarges the defects within the organic layer; the diameter of the islands increases with the number of potential excursions to positive potentials. Second, the surface cleaning step itself gives rise to some island structures (21). This phenomenon is probably the result of a slight roughening of the Au surface in the defect regions. Similar roughening occurs on naked Au electrodes (16).

Images of Au surfaces obtained after thiol adsorption and electrochemical cleaning, but prior to Cu UPD, indicate that the height and number density of islands is reduced compared to images obtained after Cu UPD. These results, in conjunction with the electrochemical data shown in Fig. 1 and Auger electron spectroscopy which indicates the presence of Au, Cu, S, and C on the Au (111) surface following Cu UPD, strongly suggest that full development of the island structures shown in Fig. 2 requires the presence of Cu within the defect sites. However, the precise chemical and morphological nature of the islands requires a more detailed analysis than we can provide at the present time.

Figure 3 shows a plot of the number of islands per unit area, which we correlate to the total number of defects originally present within the organic layer, as a function of immersion time in the $CH_3(CH_2)_{17}SH$ deposition solution. The number density of islands is obtained by estimating the number of islands in three representative $200 \times 200 \text{ nm}$ regions on at least two

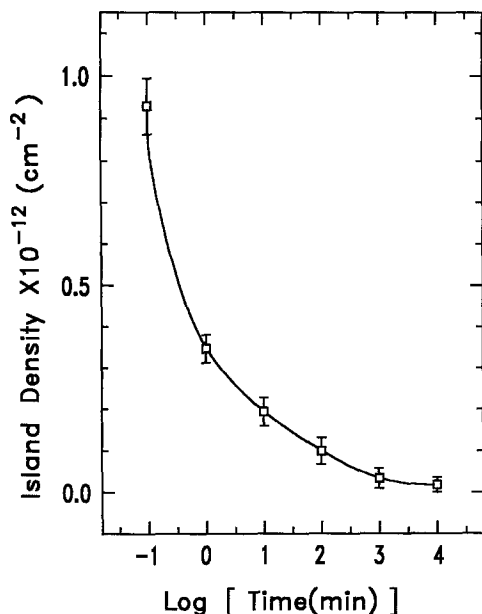


Fig. 3. Plot of island density as a function of the time allotted for $\text{CH}_3(\text{CH}_2)_{17}\text{SH}$ deposition. Densities were determined by counting the Cu islands present in three 200×200 nm regions of a Au (111) facet. The error bars represent one standard deviation from the mean number density obtained from at least three regions on each of two independently prepared surfaces.

independently prepared Au (111) surfaces. The error bars represent one standard deviation from the experimentally determined mean value of these measurements. The important result is that the number of islands decreases as a function of the time allotted for self-assembly.

It is interesting to compare the self-assembly kinetics presented here with those obtained by Whitesides *et al.* (4). They have asserted that assembly proceeds in two steps: rapid adsorption of an imperfect monolayer followed by a slower process of additional adsorption and consolidation. They concluded that limiting ellipsometric and contact angle properties were obtained after 10^3 min and our results, Fig. 3, are in general agreement with this assessment. However, the methodology described here is clearly more sensitive to small changes in monolayer morphology since very subtle changes are still evident even after prolonged immersion in the *n*-alkylthiol solution.

Careful examination of Fig. 2, especially frame f, shows that there are features present within the *n*-alkylthiol framework that do not contain island structures. High resolution STM images indicate these holes are about 0.5 nm deep and between 2 and 5 nm in diameter. At present, the origin of these features is uncertain; however, we speculate that they result from defects within the organic layer. An obvious question concerns the absence of Cu within these small defect sites. One possibility is that the defects exist only near the Au surface while the top portion of the monolayer remains more or less intact preventing diffusion of Cu^{2+} to the Au surface. Alternatively, the defects may penetrate the organic layer completely, but still restrict mass transfer of Cu^{2+} because the environment within the pores is somewhat hydrophobic. Resolution of this question awaits a complete STM analysis of the organic adlayer with particular attention placed on the distance between the STM tip and the Au substrate during imaging.

Conclusions

To summarize, we have shown that it is possible to use a combination of electrochemical methods and STM to measure

the number density of nanometer-scale defects contained within a self-assembled *n*-alkylthiol monolayer as a function of time. The rate of defect disappearance measured by the UPD/STM technique is in general agreement with previous results obtained using techniques that rely upon the macroscopic characteristics of the organic surface (4).

Experiments designed to elucidate the precise chemical and morphological nature of the island structures are in progress. Additional information about the organic defect regions themselves and the spatial relationship between the STM tip, the organic monolayer, and the substrate surface will be required before all of the results presented here can be fully interpreted.

Acknowledgments

This work is supported by the National Science Foundation (CHE-90146566) and by a grant from Digital Instruments, Incorporated (Santa Barbara, California). R.M.C. gratefully acknowledges a Society of Analytical Chemists of Pittsburgh Starter Grant Award. We thank A. J. Ricco and Wayne Buttry of Sandia National Laboratories for Auger electron spectroscopic analyses.

Manuscript submitted March 15, 1991; revised manuscript received May 24, 1991.

The University of New Mexico assisted in meeting the publication costs of this article.

REFERENCES

1. J. D. Swalen, D. L. Allara, J. D. Andrade, E. A. Chandross, S. Garoff, J. Isreelachvili, T. J. McCarthy, R. Murray, R. F. Pease, J. F. Rabolt, K. J. Wynne, and H. Yu, *Langmuir*, **3**, 932 (1987).
2. R. G. Nuzzo and D. L. Allara, *J. Am. Chem. Soc.*, **105**, 4481 (1983).
3. R. G. Nuzzo, L. H. Dubois, and D. L. Allara, *ibid.*, **112**, 558 (1990), and references therein.
4. C. D. Bain, E. B. Troughton, Y.-T. Tao, J. Evall, G. M. Whitesides, and R. G. Nuzzo, *ibid.*, **111**, 321 (1989), and references therein.
5. C. E. D. Chidsey and D. N. Loiacono, *Langmuir*, **6**, 682 (1990); and references therein.
6. H. O. Finklea, D. A. Snider, and J. Fedyk, *ibid.*, **6**, 371 (1990), and references therein.
7. H. Lee, L. J. Kepley, H.-G. Hong, S. Akhter, and T. E. Mallouk, *J. Phys. Chem.*, **92**, 2597 (1988), and references therein.
8. J. Sagiv, *Isr. J. Chem.*, **18**, 346 (1979).
9. J.-H. Kim, T. M. Cotton, and R. A. Uphaus, *J. Phys. Chem.*, **92**, 5575 (1988).
10. J. Pemberton *et al.*, *J. Am. Chem. Soc.*, In press.
11. M. D. Porter, T. B. Bright, D. L. Allara, and C. E. D. Chidsey, *ibid.*, **109**, 3559 (1987).
12. R. G. Nuzzo, L. H. Dubois, and D. L. Allara, *ibid.*, **112**, 558 (1990), and references therein.
13. R. Thomas, L. Sun, R. M. Crooks, and A. J. Ricco, *Langmuir*, **7**, 620 (1991).
14. A recent report has discussed tunneling microscopy of defect-free self-assembled overlayers on Au (111) substrates: C. A. Widrig, C. A. Alves, and M. D. Porter, *J. Am. Chem. Soc.*, **113**, 2805 (1991).
15. T. Hsu, *Ultramicroscopy*, **11**, 167 (1983).
16. D. J. Trevor, C. E. D. Chidsey, and D. N. Loiacono, *Phys. Rev. Lett.*, **62**, 929 (1989).
17. Digital Instruments, Inc., Santa Barbara, CA.
18. C. E. D. Chidsey, G.-Y. Liu, P. Rowntree, and G. Scoles, *J. Chem. Phys.*, **91**, 4421 (1989).
19. M. S. Zei, G. Qiao, G. Lehmpfuhl, and D. M. Kolb, *Ber. Bunsenges. Phys. Chem.*, **91**, 349 (1987).
20. J. J. Magda, M. Tirrell, and H. T. Davis, *J. Chem. Phys.*, **83**, 1888 (1985).
21. We thank one of the reviewers for suggesting this experiment.